A New Way To Understand Quaternary Structure Changes of Hemoglobin upon Ligand Binding On the Basis of UV−Resonance Raman Evaluation of Intersubunit Interactions

ARTICLE *in* JOURNAL OF THE AMERICAN CHEMICAL SOCIETY · JUNE 2011

Impact Factor: 12.11 · DOI: 10.1021/ja111370f · Source: PubMed

3 AUTHORS, INCLUDING:

Masako Nagai
Hosei University
69 PUBLICATIONS **873** CITATIONS

SEE PROFILE

JACS
JOURNAL OF THE AMERICAN CHEMICAL SOCIETY

ARTICLE

pubs.acs.org/JACS

A New Way To Understand Quaternary Structure Changes of Hemoglobin upon Ligand Binding On the Basis of UV-Resonance Raman Evaluation of Intersubunit Interactions

Shigenori Nagatomo,[†] Masako Nagai,[‡] and Teizo Kitagawa*[,§]

[†]Department of Chemistry, University of Tsukuba, Tsukuba, Ibaraki 305-8571, Japan

[‡]Research Center for Micro-Nano Technology, Hosei University, Koganei, Tokyo 184-0003, Japan

[§]Picobiology Institute, Graduate School of Life Science, University of Hyogo, 3-2-1 Kouto, Kamigori, Ako-gun, Hyogo 678-1297, Japan

Supporting Information

ABSTRACT: The single residue vibrational spectra of tryptophan (Trp) and tyrosine (Tyr) residues in human adult hemoglobin (HbA), which play important roles in cooperative oxygen binding, were determined for the deoxy and CO-bound forms by applying UV resonance Raman spectroscopy to various variant Hbs. It was found that Trpβ37, Tyrα42, Tyrα140, and Tyrβ145 at the $\alpha^1-\beta^2$ subunit interface underwent transitions between two contact states (named as T and R) upon ligand binding, while Trpα14, Trpβ15, and Tyrβ35 displayed little changes. The corresponding spectral changes were identified only for the $\alpha_2\beta_2$ tetramer, but not the isolated α and β chains in the oligomeric forms, and therefore were exclusively attributed to a quaternary structure change. Ligand binding as well as allosteric effectors and pH altered only the number of the T-contacted Tyr and Trp residues without varying the two contact states themselves. A new method to semiquantitatively evaluate the amount of T-contacted Tyr and Trp residues in a given liganded form is here proposed, and with it a quaternary structure was determined for various symmetrically half-liganded forms obtained with ligand−hybrid, metal−hybrid, and valency−hybrid Hbs. It was found that ligand binding to the α or β subunits yielded different subunit contacts and that the contact changes of the Trp and Tyr residues were not always concerted. The contact changes at the $\alpha^1-\beta^2$ ($\alpha^2-\beta^1$) interface are correlated with the proximal strain exerted on the Fe−His(F8) bond, which is noted to be much larger in the α than β subunits in the $\alpha_2\beta_2$ tetramer.

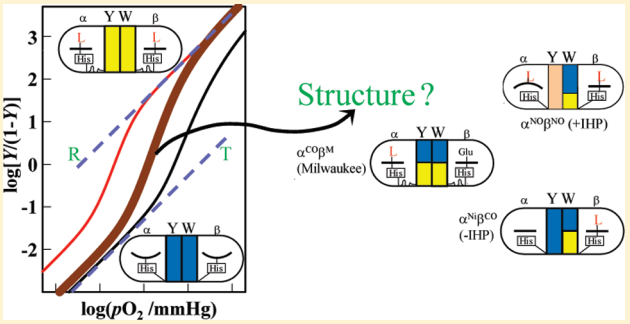

INTRODUCTION

The characteristic property of hemoglobin (Hb) is cooperativity in O_2 binding,[1a−1c,2] which has been extensively investigated as a model of general allosteric proteins.[3] Human adult Hb (HbA) is composed of two α (141 residues) and two β (146 residues) subunits, forming an $\alpha_2\beta_2$ tetramer, in which the ($\alpha^1\beta^1$) dimer is correlated with ($\alpha^2\beta^2$) dimer by 2-fold symmetry axis.[4] Each subunit has one protoheme covalently bound to a histidine residue of the F helix (His F8). Irrespective of whether it is the α or β subunit, the isolated chains stay in an oligomeric form but exhibit no cooperativity in O_2 binding, and have properties similar to those of myoglobin (Mb). X-ray crystallographic studies of HbA have demonstrated the presence of two distinct quaternary structures that correspond to the low-affinity (tense or T) and high-affinity (relaxed or R) states, which have practically been determined for the unliganded form (deoxyHb) and CO-bound form (COHb), respectively.[1b,1c]

Classically, the cooperative O_2 binding of Hb has been explained in terms of the two-state model, which assumes an equilibrium between the two quaternary states (T and R) in individual steps of ligand binding (MWC model),[3] or a sequential change model, which assumes successive structural changes at each step of ligand binding (KNF model).[5] The KNF model accounts for O_2 binding with four binding constants (K_1-K_4) of each step and explains the positive cooperativity by the fact of $K_1 < K_2 < K_3 < K_4$. This model is phenomenologically correct, although it provides no structural insight into general allosteric proteins. In contrast, the MWC model elegantly accounts for the cooperative O_2 binding with only three independent parameters (K_T, K_R, and L) for HbA under various solvent conditions.[2] This theory postulates the concerted change of the four subunits, although there has been no experimental evidence for this. It is noted that neither model distinguishes between the α and β subunits, although their structural differences have been pointed out.[6,7a,7b] In addition to the typical two structures, several quaternary structures have been found in crystallography,[8−10] and solution studies including NMR,[7a,7b,11a−11c] Raman,[12a−12c,13a,13b]

Received: December 17, 2010

   dx.doi.org/10.1021/ja111370f | J. Am. Chem. Soc. XXXX, XXX, 000–000

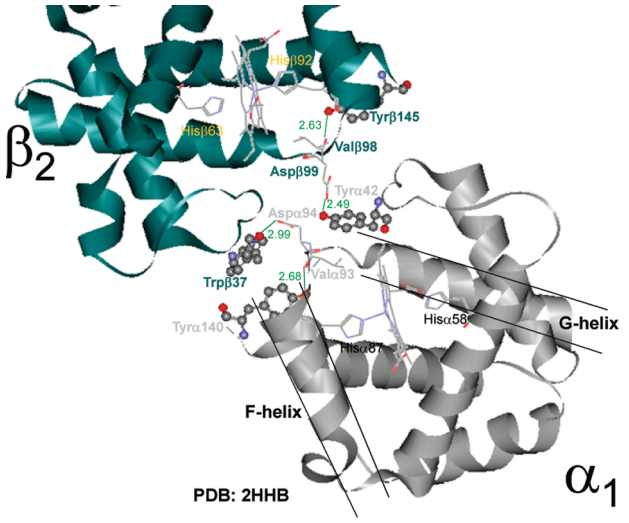

Figure 1. Intersubunit interactions of deoxyHbA at the interface between the α^1 and β^2 subunits revealed by X-ray crystallography (ref 44, PDB: 2HHB). Tyrα42 is hydrogen bonded to Aspβ99, and Trpβ37 to Aspα94 of the G-helix. Tyrα140 (HC2) is hydrogen bonded to Valα93. These hydrogen bonds are absent in the liganded form. The F-helix contains the proximal His (F8).

kinetics,[14] and sol−gel fixation.[12b,12c,15] To account for inadequacies of the original MWC and KNF models, several new models have been proposed including the global allostery,[16a] molecular code,[17a−17d] tertiary two states,[18] and two T states.[15,19]

In a microscopic view, on the other hand, there should be eight intermediates in ligand binding to ($\alpha^1\beta^1\alpha^2\beta^2$) tetramer. Ackers and colleagues determined the free energy changes for 16 possible binding reactions and pointed out that only six reactions are accompanied by the T to R quaternary structure change.[17c] The intersubunit linkage within ($\alpha^1\beta^1$) dimer (also in $\alpha^2\beta^2$ dimer, but deleted hereafter) is basically composed of hydrophobic interactions and is stronger than the interdimer interactions, which are basically composed of hydrogen bonds and salt-bridges as seen for the $\alpha^1-\beta^2$ (and $\alpha^2-\beta^1$) subunit interface. Although cooperativity is present within the ($\alpha^1\beta^1$) dimer,[17a] structural changes upon ligand binding within the dimer are relatively small.[13b,20] X-ray crystallography demonstrated the presence of large structural differences between the typical T and R states in the $\alpha^1-\beta^2$ subunit interface rather than that within the ($\alpha^1\beta^1$) dimer.[6] The $\alpha^1-\beta^2$ subunit interface is illustrated in Figure 1, where realignments of the hydrogen bonds and salt-bridges take place upon ligand binding.[6] The ^{1}H NMR signal of Tyrα42, which is free in the R state but is hydrogen-bonded with Aspβ99 in the T state, has served as a practical marker of the quaternary structure.[7a]

It has been found that the Raman spectra of the Tyr and Trp residues are extremely sensitive to hydrogen bonding and environment.[21a−21e] Ultraviolet resonance Raman (UVRR) spectroscopy is a unique technique for observing the vibrational spectra of such aromatic residues selectively and has been applied to the structural analysis of Hb.[22−30] Because of recent technical developments, the combination of site-specific mutagenesis with calculations of difference spectra has enabled the extraction of the spectra of single residues of the native tetramer. In this study, we perform the extraction of single residue spectra of Trp and Tyr in unliganded HbA (deoxyHbA) and CO-bound HbA (COHbA) and determine the contributions of individual residues to the whole spectral change upon ligand binding. Furthermore, we propose a new evaluation method regarding how much of these residues are in T (or R) contact in the symmetrically half-liganded Hbs on the basis of their observed UVRR spectra.

MATERIALS AND METHODS

HbA was purified from fresh human blood by preparative isoelectric focusing electrophoresis using 5% Ampholine (pH 6−9).[23a] DeoxyHb and COHb were prepared by adding sodium dithionite (1 mg/mL) to oxyHb after replacement of the inside air of the sample tube with N_2 and CO, respectively. NOHb was obtained by addition of NO, which had been in advance passed through 1 M NaOH solution, to deoxyHb. A method for the preparation of the isolated α-NO chain was described elsewhere,[16b] and the concentration of α-NO chain was calculated using extinction coefficients of 13.57 and 13.83 mM^{-1} cm^{-1} at 572 and 544 nm, respectively, at pH 7.0. The half-ligated Hb, $\alpha^{NO}\beta^{deoxy}$, was obtained through the addition of a small amount of sodium dithionite to a mixed solution of the α-NO chain and β-O_2 chain. It was reported previously[16b] that the affinity of NO for the α-hemes of Hb is more than 100-fold stronger than that for the β-hemes under physiological conditions. The NO−CO mixed-liganded Hb, $\alpha^{NO}\beta^{CO}$, was prepared by adding CO to $\alpha^{NO}\beta^{deoxy}$. No migration of NO from the α to the β subunit during the experiments was confirmed with EPR. Integrity of all samples including $\alpha^{NO}\beta^{deoxy}$, $\alpha^{NO}\beta^{CO}$, and NOHb ($\alpha^{NO}\beta^{NO}$) due to exposure to the UV laser light even at pH 5.5 was carefully checked by inspecting a possible change in the visible absorption spectrum before and after the measurements of UVRR spectra.

To get single residue spectra, we measured a spectrum of variant Hb, in which a given Tyr or Trp residue is replaced with a UVRR-inactive residue. The difference spectrum between HbA and variant Hb provided the spectrum of the particular residue which was replaced. This was determined with each of the deoxy and CO forms, and then their difference spectrum was calculated. The solution conditions were adjusted to exhibit a Hill coefficient larger than 2, particularly for the variant Hbs. For Tyrα42, Tyrβ35, Trpα14, Trpβ15, and Trpβ37, recombinant Hbs (Tyrα42→Ser),[23e] (Tyrβ35→Thr),[23b] (Trpα14→Leu),[23d] (Trpβ15→Leu),[23d] and (Trpβ37→His)[23e] were used. For Tyrα140 and Tyrβ145, Hb Rouen (Tyrα140→His)[23b] and des-(Hisβ146,Tyrβ145) Hb[23b] were used, respectively. The preparations and properties of the Ni−Fe hybrid Hb,[25b] NO−CO ligand hybrid Hb,[25a] and natural valency-hybrid Hbs (Hb M)[25c,29a] were reported previously.

The 235 nm excited UVRR spectra were obtained as previously reported.[29b] Briefly, the Raman excitation light (235 nm) was the second harmonic of an excimer laser-excited dye laser (470 nm), and the laser power at the sample point was 15 μJ/pulse. The scattered light was dispersed by an asymmetric double-spectrometer (Spex1404) in which the first and second steps were 500 nm-blazed holographic gratings with 2400 and 1200 grooves/mm, and used in the first and second order, respectively, to reject visible stray light, and was detected with an intensified photodiode array (IPDA, Hamamatsu, PC-IMD/C5222-0110G). The spectral resolution was 0.8 cm^{-1}. Approximately 150 μL of the 200−400 μM (in heme) Hb solution was put into a spinning cell having a stirring function. The sample was replaced with a fresh one every 5−10 min, and the total exposure time to obtain one spectrum was approximately 1 h. The UVRR spectra of the variant and HbA were measured under identical experimental conditions at the same time for the deoxy and CO forms. All samples contained a common amount of sulfate ions, which yielded a band at 982 cm^{-1}. This band was used as an internal intensity standard for the normalization of Raman spectra.[31a] Raman shifts were calibrated with cyclohexane.

dx.doi.org/10.1021/ja111370f |J. Am. Chem. Soc. XXXX, XXX, 000–000

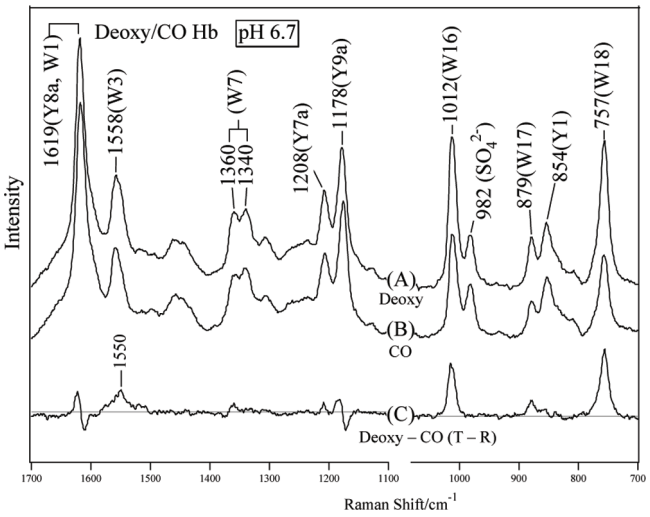

Figure 2. UVRR spectra of deoxHbA (A) and COHbA (B) at pH 6.7 and their difference spectrum (C). Excitation: 235 nm.

RESULTS AND DISCUSSION

UVRR Spectra of Native HbA. Typical UVRR spectra of deoxy- (A) and COHbA(B) excited at 235 nm in the frequency range from 1700 to 700 cm^{-1} are shown in Figure 2. The Raman bands of Tyr and Trp are marked by Y and W, respectively, followed by their mode number.[21a−21e] The band at 982 cm^{-1} arises from the SO_4^{2-} ions present as an internal intensity standard. The deoxy-minus-CO difference spectrum of HbA was digitally obtained, as shown by trace C, which serves as the standard in reference to the T − R difference spectrum.

In the raw spectra, the intensities of the W3, W16, W17, and W18 bands of Trp are weaker in COHbA than in deoxyHbA, while the peak positions remain unaltered. Accordingly, positive peaks appear in trace C. For the Tyr bands, however, the frequencies of the Y8a and Y9a bands are lower in COHbA than in deoxyHbA, and, therefore, differential patterns are evident in trace C, although Y7a exhibits a simple intensity change. These spectral differences arise from certain alterations in hydrogen bonding and the surrounding hydrophobicity of the Trp and Tyr residues upon ligand binding.[21e] The difference spectrum was unaltered by the addition of inositol hexa-phosphate (IHP).

The direct reason for the intensity increase of the Trp bands of deoxyHb is ascribed to a shift of the B_b absorption maximum to a longer wavelength, and, as a result, the wavelength difference between the Raman excitation light (235 nm) and absorption maximum of the B_b band becomes smaller, and thus the Raman resonance effect increases in deoxyHbA rather than COHbA. Such a shift of the B_b band is generally caused by an increase of hydrophobicity around the indole ring[31b] or the formation of a hydrogen bond at the indole NH site in a hydrophobic environment.[22a]

It is empirically known that W3 frequency is correlated with the $C_2-C_3-C_\beta-C_\alpha$ torsion angle of Trp residues in nonheme proteins,[21d] and the correlation curve was confirmed for Trp7 of Mb.[29c] On the basis of the curve, Rodgers et al.[22a,22b] and Hu and Spiro[27a] pointed out that the dihedral angle of the indole ring of Trpβ37 (92°) is smaller than that of Trpα14 (122°) and Trpβ15 (115°) in oxyHb, and, accordingly, the W3 frequency of Trpβ37 is lower than the others. Therefore, the difference peak in (C) at 1550 cm^{-1} is ascribed to Trpβ37, and its intensity must be stronger in the deoxy- than CO-form. The broad feature of the bandwidth would mean the wider distribution of the torsion angles in the deoxy- than in the CO-form.

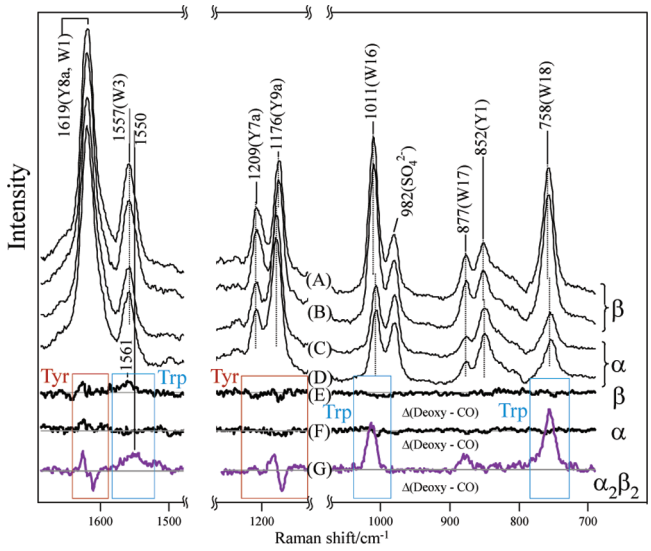

Figure 3. UVRR spectra of the deoxy- (A and C) and CO-forms (B and D) of isolated chain oligomers. Spectra A and B and spectra C and D represent the spectra of the β and α chains, respectively, and traces E and F represent the deoxy-minus-CO difference spectra of the isolated β and α chains, respectively. The deoxy-minus-CO difference spectrum of HbA ($\alpha_2\beta_2$) is delineated by (G) for comparison.

UVRR Spectra of Isolated Chains. To determine how much of these spectral changes are caused by a quaternary structure change of the $\alpha_2\beta_2$ tetramer, the isolated chains were examined, and the results are shown in Figure 3. The RR bands of Trp are stronger for the β chain than for the α chain due to the difference in the number of residues (2 for β and 1 for α). The peak frequencies of the W16 and W18 bands are slightly different between the isolated α and β chains. The Tyr spectrum of the isolated β chain also differs from that of the isolated α chain. The frequency of the Y9a band of the β-deoxy chain is lower than that of the α-deoxy chain by 4 cm^{-1}, meaning that the surroundings of Tyr in the α-deoxy chain are slightly more hydrophobic on average than those in the β-deoxy chain.

The deoxy-minus-CO difference spectra of the isolated chains are delineated by spectra E and F in Figure 3 for the β and α chains, respectively. There are no recognizable peaks in spectra E and F except for small features due to the Trp W3 band at 1561 cm^{-1} and Tyr Y9a band at 1176 cm^{-1} for the isolated β chain (E). The W3 feature indicates that the torsion angle around the $C_2-C_3-C_\beta-C_\alpha$ linkage of the Trpβ37 is slightly changed by a tertiary structure change upon ligand binding. Spectrum E exhibits a small differential pattern for Y9a, suggesting that a part of Tyr residues in the β subunit undergoes a tertiary structure change upon ligand binding. Although the intensity of differential pattern is much smaller than that of the native tetramer shown with Figure 3G, its center is located within the positive peak of Figure 3G.

Thus, it is stressed here that the frequencies and intensities of Tyr and Trp residues are almost unaltered by CO binding to the isolated α and β oligomers, although it had been anticipated that ligand binding to a heme induced a tertiary structure change from t to r within a subunit.[32] The corresponding deoxy-minus-CO

dx.doi.org/10.1021/ja111370f |J. Am. Chem. Soc. XXXX, XXX, 000–000

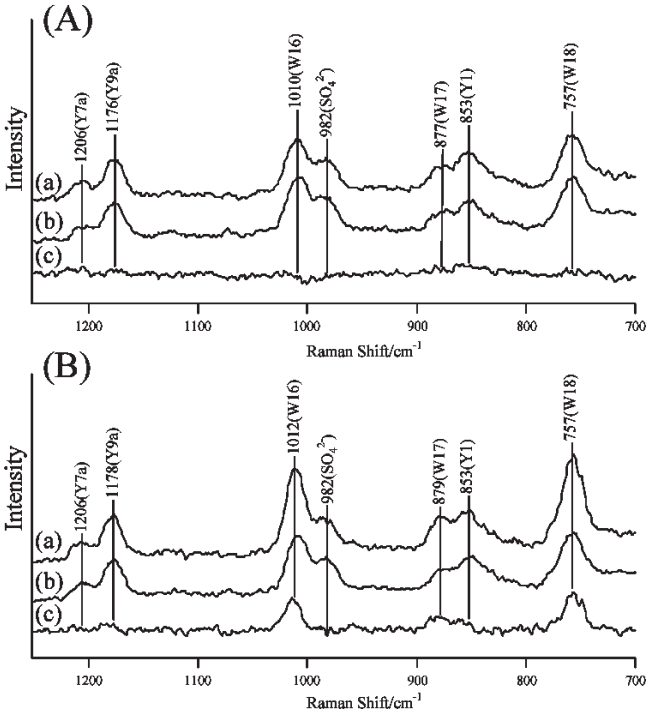

Figure 4. Comparison of the spectra of native tetramer with those of the digital sum of the spectra of isolated chains and their differences. (A) CO-form, (a) native tetramer, (b) digital sum of the isolated α and β chains, (c) difference, (a) − (b). (B) deoxy-form, (a) native tetramer, (b) digital sum of the isolated α and β chains, (c) difference, (a) − (b). The spectral intensities of the isolated chains are multiplied by 0.5 to adjust the intensity of the internal standard (982 cm^{-1}).

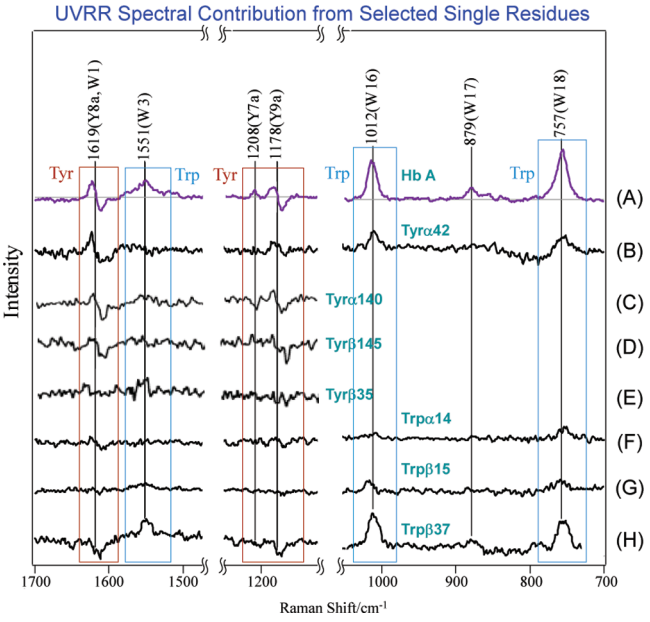

Figure 5. The extracted deoxy-minus-CO difference UVRR spectra of aromatic single residues of Hb: Tyrα42 (B), Tyrα140 (C), Tyrβ145 (D), Tyrβ35 (E), Trpα14 (F), Trpβ15 (G), and Trpβ37 (H). Trace A shows the deoxy-minus-CO difference spectrum of native Hb (HbA) represented with the same ordinate scale as in (B)−(H). Because the digitally obtained native-minus-variant difference spectra are expected to provide the contribution from the replaced residue to the whole spectra, the single residue spectra were extracted using the spectra of the corresponding variant Hbs shown in Figure SI 1 (B−H) and of HbA (A) given in the Supporting Information.

difference spectrum of native tetramer, which is reproduced at the bottom (G) using the same ordinate scale as the other traces (E and F) for comparison, definitely results from the changes of the subunit contacts upon ligand binding.

According to the X-ray crystallographic study,[6] the intrasubunit hydrogen bonds between Tyrα140 and Valα93 and between Tyrβ145 and Valβ98 are appreciably changed in length by CO binding to native Hb. These changes are recognizable in the UVRR spectra only for the native Hb, not for the isolated-chain oligomers, and therefore should be regarded as quaternary-associated intrasubunit changes. Accordingly, it is concluded that the structural alterations in the surroundings of Tyr and Trp resulting from the simple tertiary structure change upon ligand binding are much smaller than those due to quaternary structure change.

To determine whether the spectral difference between the native tetramer and the oligomers of isolated chains lies in the deoxy or CO forms, the spectra of native tetramer are compared to the digital sum of spectra of isolated α and β chains for each of the deoxy and CO forms in Figure 4. The digital sum of spectra of the α-CO and the β-CO chains (A-b) closely coincides with the spectrum of COHbA (A-a) as shown by no features in their difference spectrum (A-c). However, there is an evident difference between the corresponding digital sum of the α-deoxy and β-deoxy chains (B-b) and the spectrum of deoxyHbA (B-a) as demonstrated by their difference spectrum (B-c). It is puzzling why the difference peak of Y9a is so small in Figure 4B-c as compared to that in Figure 3G, but the directions of change are alike in both spectra. Presumably, it is due to the fact that a small frequency shift due to a tertiary structure change of β subunit occurs (see Figure 3E), and its center frequency is within the positive peak of native tetramer (Figure 3G). One of the possible interpretations is that a part of Tyr residues adopts a t-like tertiary structure in the deoxy state of isolated β chain oligomer. However, the difference spectrum, Figure 4B-c as a whole, exhibits close similarity to the T-minus-R difference spectrum shown in Figure 3G, and it would be caused by unique environments of the Trp and Tyr residues in the T state of the $\alpha_2\beta_2$ tetramer. Accordingly, these are ascribed to T-contact of these residues, which are distinct from those in the CO form, defined as R-contact. In other words, most of the Trp and Tyr residues in isolated chain oligomers are considered to be in nearly R-contacts in both the deoxy and the CO forms.

UVRR Spectra of Mutant Hbs. To elucidate the contributions from the individual Trp and Tyr residues to the difference spectrum in Figure 3G, the variant Hbs were examined. The deoxy-minus-CO difference spectra of the variant Hbs are shown in Figure SI 1 in the Supporting Information. The spectrum of a given single residue was extracted by a difference calculation, native HbA-minus-variant Hb (Figure SI 1), and the deoxy-minus-CO difference spectra of single residues thus obtained are depicted in Figure 5 for Tyrα42 (B), Tyrα140 (C), Tyrβ145 (D), Tyrβ35 (E), Trpα14 (F), Trpβ15 (G), and Trpβ37 (H). For comparison, the corresponding difference spectrum of HbA is depicted as (A) on the same ordinate scale. It is evident that the main changes of Trp bands arise from Trpβ37, while the main changes of the Tyr bands arise from Tyrα42, Tyrα140, and Tyrβ145. The contributions from Tyrβ35, Trpβ15, and Trpα14

dx.doi.org/10.1021/ja111370f |J. Am. Chem. Soc. XXXX, XXX, 000–000

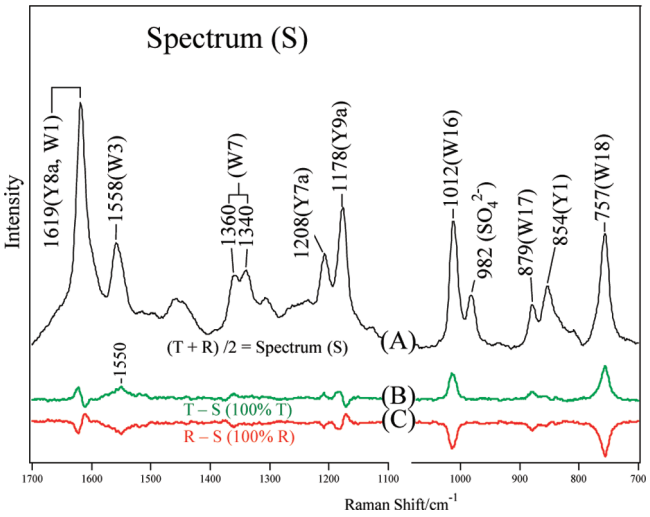

Figure 6. The newly defined spectrum (S), which is the average of the spectra of deoxyHbA (Figure 2A) and COHbA (Figure 2B). The digitally obtained difference spectra of the deoxyHbA − spectrum (S) and COHbA − spectrum (S) are delineated by traces B and C, respectively, which indicate the states of the 100%T and 100%R in the difference spectra presented in this study.

are negligible. Tyrβ35 is involved in the H-bond with Hisα122 in the ($\alpha^1\beta^1$) dimer in both deoxy and CO-forms judging from the $^1H/^2H$ exchange rate, although the H-bond is more stabilized in the CO form.[33a,33b] Trpβ15 and Trpα14 are involved in the A−E interhelical H-bonds, and the present results are compatible with the fact that mutations of their H-bonding counter residues brought about no significant effect on cooperativity.[13b]

It is apparent that some of the Tyr bands appear in the spectrum of Trpβ37 and some of the Trp bands appear in the spectrum of Tyrα42. This is presumably due to the fact that Tyrα42 is placed in the proximity of Trpβ37 (see Figure 1), and therefore removal of one hydrogen bond affects a state of nearby residues. This does not disturb the assignment but rather supports the present considerations. Note that the quaternary structure-sensitive Trp and Tyr residues have two alternative states represented by the deoxy (T-contact) and CO forms (R-contact). Trpβ37 and Tyrα42 at the α^1–β^2 (and α^2–β^1) subunit interface are the main players, while Tyrα140 and Tyrβ145 undergo quaternary-associated intrasubunit changes. Spiro and co-workers[27c] pointed out that the change of Trpβ37 in the hinge region takes place dynamically earlier than that of Tyrα42 in the switch region in the R to T transition. Other Tyr and Trp residues are almost insensitive to the quaternary structure change.

New Method for Evaluation of Quaternary Structure of HbA. Structural depictions expected for the KNF and MWC models are distinct for the half-ligated Hb. Therefore, we examined the contact states of Tyr and Trp residues in symmetric half-liganded forms, in which two ligands are bound either to the α or to the β subunits. Such a state should be an average of deoxyHbA and COHbA in the simplified KNF model, but cannot be purely produced in practice with ordinary Hbs due to cooperativity present. Therefore, we used modified Hbs. For easy judgment on how much the T (or R) contacts of Tyr and Trp are contained in a given half-liganded Hb, we propose a new evaluation method here. For this purpose, the spectrum (S) is defined as the average of T and R; spectrum (S) = (deoxyHbA + COHbA)/2 and is delineated by Figure 6A. For an observed spectrum of a given species, which is normalized with the 982 cm^{-1} band of SO_4^{2-} ions, its difference against the spectrum (S) is calculated. The difference spectra of deoxyHbA (Figure 2A) and COHbA (Figure 2B) against the spectrum (S) are calculated as shown by traces B and C in Figure 6. Traces B and C represent the 100%T and 100%R spectra, respectively, and will be used as a reference hereafter.

This treatment is mathematically equivalent to represent a spectrum of a half-liganded state as the following difference spectrum, that is, (T − R)/2 of HbA − (deoxy − CO form) of a given half-liganded species. The intensities of difference peaks are proportional to the difference between the numbers of residues having the T and R contacts: Trpβ37 for the Trp bands and a sum of Tyrα42, Tyrα140, and Tyrβ145 for the Tyr bands. Because the abscissa corresponds to 50%T (or R), the ordinate of the Trp bands in Figure 6B is scaled from 50%T- to 100%T-contact in the positive direction for individual band maxima. In the same manner, Figure 6C represents the 100%R spectrum, and the ordinate is scaled from 50%R- to 100%R-contact in the negative direction. It is easy to quantify the relative amounts of T (or R) contact from intensities for the Trp bands, but it is not straightforward to do this for the Tyr bands partly due to the differential band shape. When the spectral pattern is of a trough-to-peak type from the lower frequency side, it denotes T, and when vice versa, R. Thus, the pattern can be qualitatively determined. Hereafter, the spectra of the symmetrically half-liganded Hbs will be represented as differences against the spectrum (S), and the spectra of 100%T (Figure 6B) or 100% R (Figure 6C) are given by green and red curves, respectively, for scaling purposes. When the behaviors of Tyr and Trp are not concerted, the appearance of the corresponding difference peaks is a combination of traces B and C in Figure 6.

Ligand Hybrid Hb. Here, $\alpha^{NO}\beta^{X}$ (X = nothing, NO, or CO) of HbA are treated. The observed spectra of $\alpha^{NO}\beta^{NO}$ (=NOHb) in the presence of IHP at pH 5.2 and in its absence at pH 6.7 are given in Figure SI 2A,B, and their differences against the spectrum (S) are depicted by traces A and B in Figure 7, respectively. In the absence of IHP, $\alpha^{NO}\beta^{NO}$ (B) gives rise to 100%R contact for both Tyr and Trp as it reproduces the red curve, but in the presence of IHP (A), Trp has nearly one-half the intensity of the green spectrum, meaning ca. 75%T contact, while Tyr retains the R-contact.

NOHb ($\alpha^{NO}\beta^{NO}$) has been extensively studied by visible absorption,[34a,35,36] EPR,[34b,37a] IR,[38] and RR spectroscopies,[37b,39,40] and it is known that the Fe−His bond of the α subunit is cleaved in the T state but not in the R state, while that of the β subunit is kept in both the T and the R states. In this study, NOHb in the absence of IHP exhibited the R structure (Figure 7B), but the addition of IHP changed the Trp contact to appreciably T, but retained Tyr contact in R (Figure 7A). Here, it should be stressed that the behaviors of Trp and Tyr bands are not concerted, meaning that the whole protein structures cannot be described by the simple two-state concept, that is, typical T and R structures, although individual Trp and Tyr residues take two alternative structures.

The raw spectra of $\alpha^{NO}\beta^{deoxy}$ in the presence of IHP at pH 5.5 and in its absence at pH 8.8 are given in Figure SI 2C,D, and the difference of spectrum C of Figure SI 2 against the spectrum (S) is depicted by trace C in Figure 7, in which both Tyr and Trp have the T-contact as shown by the green curve. The difference spectrum obtained from Figure SI 2D (not shown) for $\alpha^{NO}\beta^{deoxy}$ in the absence of IHP at pH 8.8 was very similar to that of

dx.doi.org/10.1021/ja111370f |J. Am. Chem. Soc. XXXX, XXX, 000–000

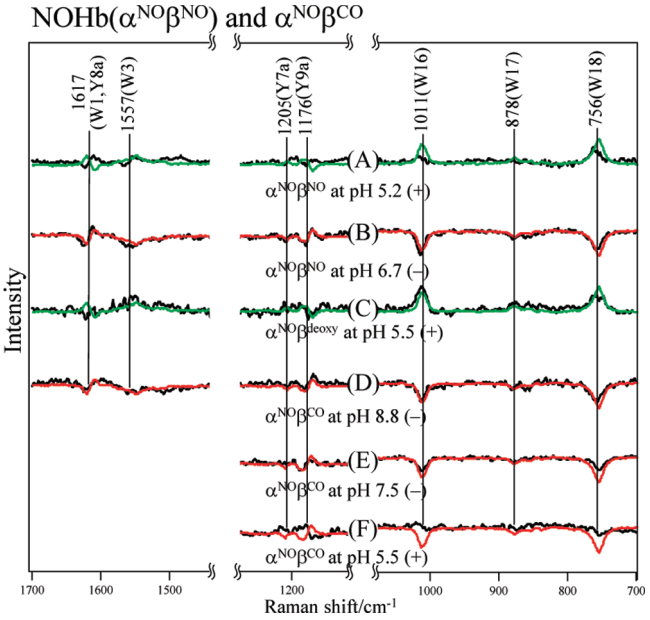

Figure 7. The UVRR difference spectra of the liganded forms of Hb against the spectrum (S). $\alpha^{NO}\beta^{NO}$ at pH 5.2 in the presence of IHP (A), $\alpha^{NO}\beta^{NO}$ at pH 6.7 in the absence of IHP (B), $\alpha^{NO}\beta^{deoxy}$ at pH 5.5 in the presence of IHP (C), $\alpha^{NO}\beta^{CO}$ at pH 8.8 in the absence of IHP (D), $\alpha^{NO}\beta^{CO}$ at pH 7.5 in the absence of IHP (E), and $\alpha^{NO}\beta^{CO}$ at pH 5.5 in the presence of IHP (F). (+) or (−) in the figure denotes the presence or absence of IHP, respectively. The 100%T- (Figure 6B) or 100%R-spectrum (Figure 6C) is overlaid with a green or red curve for easy comparison. These spectra were calculated from the corresponding raw spectra shown in Figure SI 2 (A−G) in the Supporting Information.

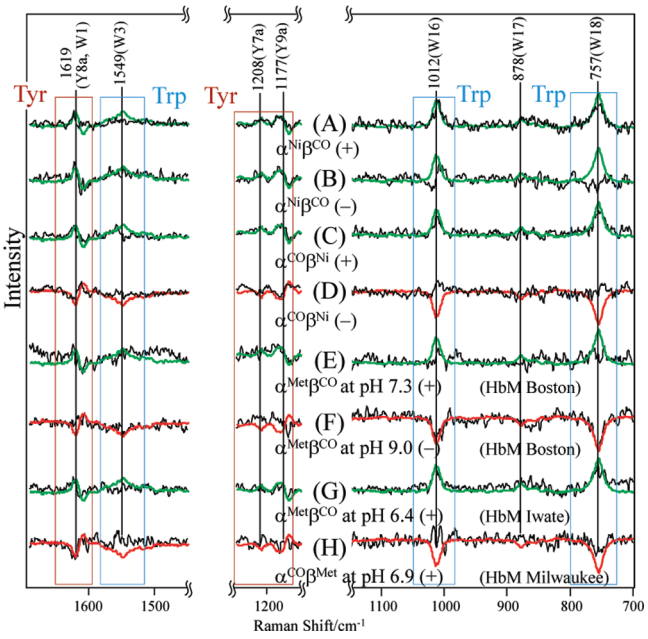

Figure 8. The UVRR difference spectra of half-liganded Hbs against the spectrum (S). $\alpha^{Ni}\beta^{CO}$ in the presence (A) and absence (B) of IHP and $\alpha^{CO}\beta^{Ni}$ in the presence (C) and absence (D) of IHP, HbM Boston $\alpha^{Met}\beta^{CO}$ at pH 7.3 in the presence of IHP (E), HbM Boston $\alpha^{Met}\beta^{CO}$ at pH 9.0 in the absence of IHP (F), HbM Iwate $\alpha^{Met}\beta^{CO}$ at pH 6.4 in the presence of IHP (G), HbM Milwaukee $\alpha^{CO}\beta^{Met}$ at pH 6.9 in the presence of IHP (H), and (+) or (−) in the figure denotes the presence or absence of IHP, respectively. Spectra A−D were calculated from the corresponding raw spectra shown in Figure SI 3, and spectra E−H were calculated from the corresponding raw spectra shown in Figure SI 4 in the Supporting Information. See the text for the definition of the spectrum (S) of the $\alpha^{Ni}\beta^{Fe}$ and HbMs. The raw spectra of the deoxy forms used for each species are also included in Figures SI 3 and SI 4. The 100%T- or 100%R-spectrum is overlaid with a green or red curve for easy comparison.

Figure 7C, meaning that the half liganded $\alpha^{NO}\beta^{deoxy}$ at both pH adopts the T structure similar to deoxyHb irrespective of the presence or absence of IHP, but when a ligand binds to its β^{deoxy} subunit, the quaternary structure is changed.

The raw spectra of the fully liganded Hb, although with different ligands, $\alpha^{NO}\beta^{CO}$ at pH 8.8 (−IHP), pH 7.5 (−IHP), and pH 5.5 (+IHP), are given in Figure SI 2E−G, and their differences against the spectrum (S) are delineated by traces D−F in Figure 7. It was confirmed by EPR that $\alpha^{NO}\beta^{deoxy}$ was stable even at pH 4.8, and no detectable ligand exchange occurred in the mixed-ligand $\alpha^{NO}\beta^{CO}$ under the present experimental conditions.[16b,25a] Trace D is almost the same as that of the 100%R depicted by the red curve, meaning that the mixed ligand Hb, $\alpha^{NO}\beta^{CO}$, in the absence of IHP at pH 8.8 adopts the R structure similar to COHb. However, the amount of R-contact in $\alpha^{NO}\beta^{CO}$ decreased when pH was lowered and became roughly 50% at pH 5.5 in the presence of IHP (F), although the difference spectrum became noisy without clear peak. Such a change was not observed for COHb ($\alpha^{CO}\beta^{CO}$).

It is briefly summarized here. The cleavage of Fe−His bond in the α subunit is correlated with a change of Trpβ37 without changes of Tyr residues. Thus, the behaviors of Trp and Tyr are not always concerted. The NO binding only to the α subunit retains HbA in the T quaternary state, but further binding of CO to the β subunit changes it to R at pH 8.8. However, it becomes 50%R at pH 5.5 in the case of NO/CO hybrid ligand, although such pH dependence was not observed for CO/CO case. It is stressed that pH change and addition of an effector, IHP, yielded only the intensity change of Trp bands with no frequency shift, although it is more complicated for Tyr.

Ni−Fe Hybrid Hb. Because CO cannot bind to the Ni subunit in Ni−Fe hybrid Hb, we can distinguish between α and β subunits in the stable two-ligand bound forms under CO-saturated conditions. Such metal hybrid Hbs were extensively used to determine the microscopic binding constants for native Hb by Ackers group.[17c,17d] The raw UVRR spectra of $\alpha^{Ni}\beta^{Fe}$ and $\alpha^{Fe}\beta^{Ni}$ in the deoxy and CO forms are given in Figure SI 3. The spectra of $\alpha^{Ni}\beta^{deoxy}$ and $\alpha^{deoxy}\beta^{Ni}$ were essentially the same as that of deoxyHb, except for the presence of weak bands due to Ni−porphyrin in the α subunit at 1620 (ν_{10}), 1380 (ν_4), and 751 (ν_{15}) cm^{-1}.[25b] This is due to the fact that Ni−porphyrin in HbA adopts the four-coordinated (4c) in the α subunit[41] and yields a weak spectrum of 4c Ni−porphyrin upon UV excitation at 235 nm, but that it adopts 5c (His-coordinated) in the β subunit and yields no Raman bands. Therefore, for cancellation of the weak Ni−porphyrin bands, the spectrum of deoxy-$\alpha^{Ni}\beta^{Fe}$ was used instead of deoxyHb for the definition of the spectrum (S) for this species. The differences of spectra of CO forms shown in Figure SI 3 against the spectrum (S) are given in Figure 8 for $\alpha^{Ni}\beta^{CO}$ (A,B) and $\alpha^{CO}\beta^{Ni}$ (C,D) at pH 6.7 in the presence (A, C) and absence of IHP (B,D). When CO is bound to the β subunit of $\alpha^{Ni}\beta^{deoxy}$, little change occurred in the UVRR spectrum, and therefore the difference spectrum (A) is almost the same as the spectrum of 100%T depicted by a green curve. In

dx.doi.org/10.1021/ja111370f |J. Am. Chem. Soc. XXXX, XXX, 000–000

the absence of IHP, however, Trp loses the T-contacts, while Tyr retains the T-contact. The spectrum of $\alpha^{CO}\beta^{Ni}$ (C) in the presence of IHP is also close to that of 100%T, but in the absence of IHP, Trp became 50%R, while Tyr is close to 100%R. Thus, the behaviors of the Tyr bands were different between $\alpha^{Ni}\beta^{CO}$ (B) and $\alpha^{CO}\beta^{Ni}$ (D) in the absence of IHP, and ligand binding to the α and β subunits resulted in appreciably different changes in the subunit contacts.

Valency Hybrid Hb. Among the five kinds of abnormal Hbs (HbMs) that cause methemoglobinaemia, methemoglobin reductase in erythrocyte is ineffective in four, because either the proximal or the distal heme-linked histidines in α or β subunits have been replaced by tyrosines. In such HbMs, the mutant subunit stays in the ferric (met) state and cannot bind CO. Therefore, under a CO atmosphere, stable symmetric two-ligand bound forms can be obtained in native proteins. In α-abnormal HbMs such as HbM Iwate (αF8His→Tyr)[42a] and HbM Boston (αE7His→Tyr),[42b] normal β-subunit has very low oxygen affinity and no cooperativity at neutral pH, indicating that the mutation of α subunit greatly influences the function of normal β subunit. HbM Milwaukee, in which Valβ67 is replaced by Glu and therefore the β heme always remains in the ferric state, has shown that the normal α subunit has also low oxygen affinity.[42c] Therefore, it is of great interest to see how large changes of quaternary structure take place in these HbMs upon ligand binding.

Because HbMs Iwate and M Boston contain additional Tyr in replacement of the distal or proximal His, the intensities of the Tyr bands are slightly larger in the raw spectra shown in Figure SI 4, although the UVRR bands of tyrosinate are not in resonance upon excitation at 235 nm.[25c,29a] Thus, the spectral patterns of deoxyHbM ($\alpha^{Met}\beta^{deoxy}$ or $\alpha^{deoxy}\beta^{Met}$) were practically identical to that of deoxyHbA. Nevertheless, to rule out any possible contribution from the additional Tyr residue, deoxyHbM was used instead of deoxyHbA in the definition of the spectrum (S), while other procedures were left unaltered.

The raw UVRR spectra of HbM Boston in the $\alpha^{Met}\beta^{deoxy}$ (A) and $\alpha^{Met}\beta^{CO}$ states (B) at pH 7.3, $\alpha^{Met}\beta^{deoxy}$ (C) and $\alpha^{Met}\beta^{CO}$ states (D) at pH 9.0, HbM Iwate in the $\alpha^{Met}\beta^{deoxy}$ (E) and $\alpha^{Met}\beta^{CO}$ states (F) at pH 6.4, and HbM Milwaukee in the $\alpha^{deoxy}\beta^{Met}$ (G) and $\alpha^{CO}\beta^{Met}$ states (H) at pH 6.9 are given in Figure SI 4. The UVRR spectrum of $\alpha^{Met}\beta^{deoxy}$ of HbM Boston (trace A in Figure SI 4) was almost the same as that of deoxyHbA. The difference spectra of COHbM Boston at pH 7.3 and 9.0, COHbM Iwate at pH 6.4, and COHbM Milwaukee at pH 6.9 against the spectrum (S) of individual species are depicted as traces E−H in Figure 8, respectively.

The $\alpha^{Met}\beta^{CO}$ of HbM Boston at pH 7.3 (E) yielded no clear peaks for Trp but the differential pattern for Tyr, indicating that Trp adopts 50% R-contacts while Tyr keeps T-contact, but at pH 9.0 (F) all Trpβ37 adopt the R-contact, as compared to the red curve (100%R), while Tyr keeps 50% T-contact. For HbM Iwate, which has abnormal α subunits similar to HbM Boston, spectrum G in Figure 8 almost overlaps with the green curve of 100% T, meaning that both Trp and Tyr in the CO forms of HbM Iwate have nearly 100% T-contact. In contrast, trace H in Figure 8 shows no peaks, indicating that both Tyr and Trp in $\alpha^{CO}\beta^{Met}$ of HbM Milwaukee adopt 50% T-contact. Thus, the changes of Tyr and Trp are not always concerted, and this is a serious challenge to the MWC model.

Correlation with the Proximal Strain. The visible laser-excited RR spectrum of native deoxyHb in the low frequency region is compared to those of the isolated chains in Figure 9. The Fe−His(F8) stretching band (ν_{Fe-His}) of deoxyHb ($\alpha_2\beta_2$) in the T state is observed in an asymmetric shape at 216 cm^{-1} (A), but the corresponding bands of the isolated chains (B,C) appear in a symmetric band shape at higher frequencies (222−223 cm^{-1}),[26b,43a,43b] while the frequencies of all of the other bands were similar between the isolated chains and the native deoxyHb. When deoxyHb was converted to the R state by removing the C-terminal residues, the ν_{Fe-His} mode appeared at 222−223 cm^{-1},[43a,43b] at the same frequency as that of deoxyMb.[26b] Spectra D and E in Figure 9 show the RR spectra of $\alpha^{deoxy}\beta^{Ni}$ and $\alpha^{Ni}\beta^{deoxy}$. The ν_{Fe-His} band appears at 201 and 216 cm^{-1} for $\alpha^{deoxy}\beta^{Ni}$ and $\alpha^{Ni}\beta^{deoxy}$, respectively, that is, at a distinctly lower frequency and weaker intensity for the α than β subunit, in agreement with the results for deoxyHbA[43b] and Zn−Fe hybrid Hb.[12a] This means that the magnitude of the strain exerted on the Fe−His bond is clearly larger in the α than in the β subunit.

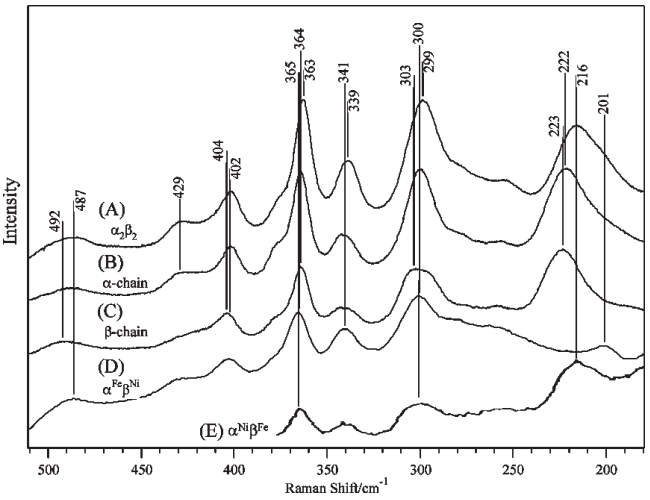

Figure 9. The 441 nm excited RR spectra of the deoxyHb (A), deoxy forms of the isolated α chain (B) and β chain (C), and deoxy forms of the Ni−Fe metal hybrid Hb, $\alpha^{Fe}\beta^{Ni}$ (D) and $\alpha^{Ni}\beta^{Fe}$ (E).

Although the isolated chains form oligomers, the interactions at the subunit surfaces never induce the proximal strain in the interior. Therefore, their ν_{Fe-His} frequencies are almost the same as that of deoxyMb.[26b] In the native $\alpha_2\beta_2$ tetramer with the T state, the intersubunit interactions shown in Figure 1 generate the proximal strain in the heme pocket of the individual subunits. When the intersubunit interactions are relaxed, the proximal strain disappears, and the ν_{Fe-His} frequency becomes the same as those of the isolated chains.[43b] Therefore, the UVRR bands and the ν_{Fe-His} serve consistently as markers of the quaternary structure at the $\alpha^1-\beta^2$ (and $\alpha^2-\beta^1$) interface. However, the present discussion is limited to the stationary states and does not cover the CO-photodissociated transient species, which yield the ν_{Fe-His} band at ∼230 cm^{-1} for the nonequilibrium planar deoxy heme.[12a]

Quaternary Structure Change of HbA upon Ligand Binding. The quaternary structure-sensitive Trp and Tyr residues have two alternative states in HbA, the R-contact and T-contact. Trpβ37 and Tyrα42 at the $\alpha^1-\beta^2$ (and $\alpha^2-\beta^1$) subunit interface are the residues most sensitive to quaternary structure changes, while Tyrα140 and Tyrβ145 undergo quaternary-associated intrasubunit changes. It is reported[27c] that the change

dx.doi.org/10.1021/ja111370f |J. Am. Chem. Soc. XXXX, XXX, 000–000

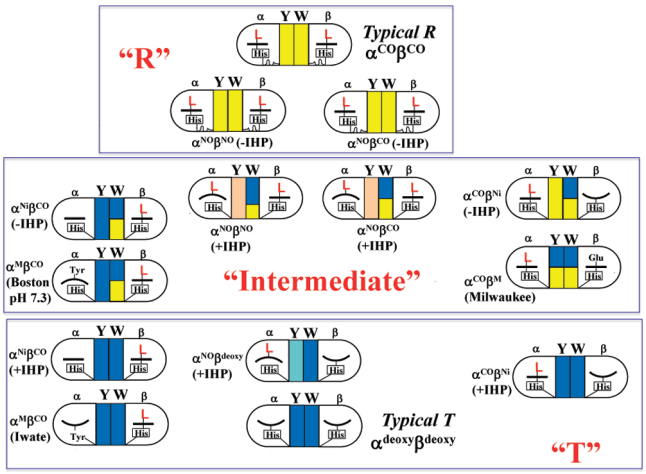

Figure 10. Illustrative representation of quaternary structures of Hb in various liganded states. The left and right circles symbolically represent the α^1 and β^2 subunits, respectively, and two squares between them mean Tyr (Y) and Trp (W) residues at the subunit contact region. The blue and yellow colors of the squares indicate the T- and R-contacts, respectively, and their areas are proportional to the relative amounts of T or R contacts. Light blue and pink mean nearly T- and R-contact, respectively. L denotes an external ligand (NO, CO, and O_2). His in a rectangle denotes the proximal (F8) histidine. A shape of heme is represented by a bar (planar) or a bowl (domed), and the Fe−His bond is represented, if present, by a short line between a heme and His. The solid lines and waved lines under the His indicate the constrained and relaxed states of the Fe−His bond, respectively. These Hbs could be categorized into three groups, "T", "intermediate", and "R", from color distribution of the contact region. When colors of both Y and W are blue, these Hbs are categorized into "T". Hbs having yellow color in both Y and W are grouped into "R". Hbs with mixed colors are grouped into "intermediate".

of Trpβ37 in the hinge region takes place dynamically earlier than that of Tyrα42 in the switch region upon the R to T transition. Other Tyr and Trp residues are almost insensitive to the quaternary structure change. We have proposed a new method to quantify the relative amount of T- (or R-) contacted residues on the basis of band intensities in the difference spectrum of a half-liganded state against spectrum (S).

Figures 7 and 8 present such difference spectra against the spectrum (S). Regarding Trpβ37, the positive and negative peaks reflect the amount of the T- and R-contacts, respectively, and the band intensities provide the number of such contacts scaled 50−100%, with the reference of the colored curve standing for 100%. For the Tyr bands, quantitative estimation is not easy, partly due to the differential patterns and partly due to the differences in sensitivities among the three Tyr residues. With this semiquantitative evaluation method, rough amounts of T (or R) contacted-Trp and Tyr residues were estimated and represented by relative areas of blue (or yellow)-colored squares for all of the examined liganded states in Figure 10, in which light blue and pink indicate nearly T- and R-contact (>70%), respectively. Intuitively, the quaternary structures of various liganded states of Hbs could be categorized into three groups on the basis of color distributions in Figure 10: "R", "intermediate", and "T".

In addition to the typical "T" state of deoxyHb, $\alpha^{Ni}\beta^{CO}$(+IHP), $\alpha^{NO}\beta^{deoxy}$(+IHP), $\alpha^{CO}\beta^{Ni}$(+IHP), and HbM Iwate-CO ($\alpha^{M}\beta^{CO}$) can be categorized into "T". The fully liganded Hbs such as $\alpha^{NO}\beta^{NO}$(−IHP) and $\alpha^{NO}\beta^{CO}$(−IHP) are grouped into the "R" in addition to the typical R of HbCO. However, the addition of IHP to these fully liganded ones causes to shift to the "intermediate", although close to "R". Half-liganded Hbs such as $\alpha^{Ni}\beta^{CO}$(−IHP) and HbM BostonCO ($\alpha^{M}\beta^{CO}$) belong to the "intermediate", although close to "T". So far, several quaternary structures of Hbs including R2,[8,12b,12c] RR2 and R3,[10] tight- and loosened-T,[12a] low-affinity T,[15,19] and T_{high}[9] have been proposed, but the present conclusion is unique regarding the first semiquantitative evaluation of the quaternary structure of half-liganded Hbs.

It is apparent from Figure 10 that the changes of the Tyr and Trp residues are not always concerted among different symmetric hybrids. This feature goes against the model based on the concerted change of all of the subunits. Furthermore, the amount of the T- or R-contacts of these residues is different between the symmetric half-liganded forms in which two ligands are bound either to the α (left side) or to the β subunits (right side). It became evident from Figure 7A that the cleavage of the Fe−His bond in the α subunit brought Trpβ37 into T-contact without changing the Tyr contact.

It is also deduced from Figure 9 that the magnitude of strain is definitely larger in the α than β subunits when the intersubunit interactions are in T-contact. The Fe−His bond-length in the α subunit changes from 216 to 194 pm upon ligand binding.[44−46] As a result of the additional movement of the Fe^{2+} ion due to the change in heme from a domed to planar structure, the movement of the N_ε of the proximal His in the α subunit is estimated to be as large as 60 pm. In contrast, the Fe−His bond-length in the β subunit changes from 209 to 207 pm.[44−46] Even after the addition of the movement of Fe^{2+}, the corresponding displacement of the N_ε of the proximal His in the β subunit upon ligand binding is estimated to be ca. 40 pm. The difference in the moving distances of the proximal His presumably causes the different effects in the subunit contacts between the ligand binding to the α and β subunits.

The ligand binding to the α subunit induces a larger displacement of F8 His(α), and thus a larger movement of the α-F helix. The movement of the F helix is communicated to the C terminal and thus to Tyrα140, which is hydrogen bonded to Valα93. Next, it induces a structural change of the next residue, Aspα94, which is hydrogen bonded to Trpβ37. Consequently, it is understandable that ligand binding to the α subunit and also the cleavage of the Fe−His bond in the α subunit alter the contact state of Trpβ37. It was noted from X-ray crystallographic analysis[9] that a change in the Fe−His bond of the β subunit is linked to Trpβ37 through bending of the ($\alpha^1\beta^1$) dimer. The rather small strain in the Fe−His bond of β subunit would result in a smaller change of Trpβ37 in the ligand binding to the β subunit than that to the α subunit. This is consistent with Noble et al.[47] who pointed out that ligand binding to the α subunit alters more sensitively Trpβ37 than that to the β subunit.

From the tendency of changes of Tyr and Trpβ37 at $\alpha^1-\beta^2$ contact, the T to R transition seems to start from the changes of Tyr, followed by Trpβ37, when ligands bind to α subunits, as seen for $\alpha^{CO}\beta^{Ni}$(−IHP). On the contrary, the change of Trpβ37 precedes the change of Tyr when ligands bind to β subunits, as seen for $\alpha^{Ni}\beta^{CO}$(−IHP) and HbM BostonCO($\alpha^{M}\beta^{CO}$). These results suggest that the changes of these aromatic residues at the $\alpha^1-\beta^2$ contact have some order and may give a new insight into a cooperative ligand binding mechanism of Hb.

It is possible to assume that the hydrogen bonds of Tyrα140 and Trpβ37 are lost but the hydrogen bond of Tyrα42 is kept.

dx.doi.org/10.1021/ja111370f |J. Am. Chem. Soc. XXXX, XXX, 000–000

This corresponds to an imperfect T structure as seen for $\alpha^{Ni}\beta^{CO}$ and HbM Boston-CO at pH 9 without IHP and may correspond to the loosened T^{12a} and $T_{High}{}^{9}$ structures. Despite the large variations in the T (or R) contacts of Tyr and Trp, which must cause affinity changes, the two states of interaction strengths of individual residues remain unaltered, and only the populations of the interacted residues are changed by pH, ligand, and/or effectors. The uniqueness of HbA seems to arise primarily from the character of α deoxy subunit in the $\alpha_2\beta_2$ tetramer.

■ ASSOCIATED CONTENT

Supporting Information. Additional figures. This material is available free of charge via the Internet at http://pubs.acs.org.

■ AUTHOR INFORMATION

Corresponding Author
teizo@sci.u-hyogo.ac.jp

■ ACKNOWLEDGMENT

This study was supported by a Grant-in-Aid for Scientific Research (no. 21350098) to T.K. from the Japan Society for Promotion of Science. We are grateful to Profs. Takashi Yonetani of the University of Pennsylvania and Tsuneshige Antonio of Hosei University for preparation and characterization of NOHb, Dr. Naoya Shibayama of Jichi Medical University for preparation and characterization of Fe−Ni hybrid Hb, Prof. Hiroshi Hori of Osaka University for EPR measurements of HbM Boston, Prof. Chien Ho of Carnegie Melon University for the gift of the *E. coli* Hb expression plasmid, pHE7, and Dr. Yayoi Aki of Kanazawa University for constructing plasmids and expressing mutant Hbs. We appreciate the gifts of blood containing abnormal Hb, from Dr. H. Sakai (HbM Iwate), Profs. R. Jagenburg (HbM Boston), A. V. Pisciotta (HbM Milwaukee), and H. Wajcman (Hb Rouen). T.K. acknowledges the support by the Global COE Program, "Picobiology: Life Science at the Atomic Level" at the Graduate School of Life Science, University of Hyogo, from MEXT, Japan.

■ REFERENCES

(1) (a) Perutz, M. F. *Mechanism of Cooperativity and Allosteric Regulation in Proteins*; Cambridge University Press: Cambridge, U.K., 1990. (b) Perutz, M. F. *Nature* **1970**, *228*, 726–739. (c) Perutz, M. F. *Annu. Rev. Biochem.* **1979**, *48*, 327–386.

(2) Imai, K. *Allosteric Effects in Haemoglobin*; Cambridge University Press: Cambridge, 1982.

(3) Monod, J.; Wyman, J.; Changeux, J. P. *J. Mol. Biol.* **1965**, *12*, 88–118.

(4) Fermi, G. *J. Mol. Biol.* **1975**, *97*, 237–256.

(5) Koshland, D. E., Jr.; Némethy, G.; Filmer, D. *Biochemistry* **1966**, *5*, 365–385.

(6) Baldwin, J.; Chothia, C. *J. Mol. Biol.* **1979**, *129*, 175–220.

(7) (a) Fung, L. W.-M.; Ho, C. *Biochemistry* **1975**, *14*, 2526–2535. (b) Ho, C. *Adv. Protein Chem.* **1992**, *43*, 153–312.

(8) Silva, M. M.; Rogers, P. H.; Arnone, A. *J. Biol. Chem.* **1992**, *267*, 17248–17256.

(9) Kavanaugh, J. S.; Rogers, P. H.; Arnone, A. *Biochemistry* **2005**, *44*, 6101–6121.

(10) Safo, M. K.; Abraham, D. J. *Biochemistry* **2005**, *44*, 8347–8359.

(11) (a) Maillett, D. H.; Simplaceanu, V.; Shen, T.-J.; Ho, N. T.; Olson, J. S.; Ho, C. *Biochemistry* **2008**, *47*, 10551–10563. (b) Lukin, J. A.; Kontaxis, G.; Simplaceanu, V.; Yuan, Y.; Box, A.; Ho, C. *Proc. Natl. Acad. Sci. U.S.A.* **2003**, *100*, 517–520. (c) Gong, Q.; Simplaceanu, V.; Lukin, J. A.; Giovannelli, J. L.; Ho, N. T.; Ho, C. *Biochemistry* **2006**, *45*, 5140–5148.

(12) (a) Samuni, U.; Juszczak, L.; Dantsker, D.; Khan, I.; Friedman, A. J.; Peréz-González-de-Apodaca, J.; Bruno, S.; Hui, H. L.; Colby, J. E.; Karasik, E.; Kwiatkowski, L. D.; Mozzarelli, A.; Noble, R.; Friedman, J. M. *Biochemistry* **2003**, *42*, 8272–8288. (b) Samuni, U.; Roche, C. J.; Dantsker, D.; Juszczak, L.; Friedman, J. M. *Biochemistry* **2006**, *45*, 2820–2835. (c) Samuni, U.; Roche, C. J.; Dantsker, D.; Friedman, J. M. *J. Am. Chem. Soc.* **2007**, *129*, 12756–12764.

(13) (a) Jayaraman, V.; Rodgers, K. R.; Mukerji, I.; Spiro, T. G. *Science* **1995**, *269*, 1843–1848. (b) Balakrishnan, G.; Tsai, C.-H.; Wu, Q.; Case, M. A.; Pevsner, A.; McLendon, G. L.; Ho, C.; Spiro, T. G. *J. Mol. Biol.* **2004**, *340*, 857–868.

(14) Gibson, Q. H. *Biochemistry* **1999**, *38*, 5191–5199.

(15) Shibayama, N.; Saigo, S. *FEBS Lett.* **2001**, *492*, 50–53.

(16) (a) Yonetani, T.; Park, S.; Tsuneshige, A.; Imai, K.; Kanaori, K. *J. Biol. Chem.* **2002**, *277*, 34508–34520. (b) Yonetani, T.; Tsuneshige, A.; Zhou, Y.; Chen, X. *J. Biol. Chem.* **1998**, *273*, 20323–20333.

(17) (a) Ackers, G. K.; Doyle, M. L.; Myers, D.; Daugherty, M. A. *Science* **1992**, *255*, 54–63. (b) Ackers, G. K.; Holt, J. M. *J. Biol. Chem.* **2006**, *281*, 11441–11443. (c) Ackers, G. K. *Adv. Protein Chem.* **1998**, *51*, 185–253. (d) Huang, Y.; Yonetani, T.; Tsuneshige, A.; Hoffman, B. M.; Ackers, G. K. *Proc. Natl. Acad. Sci. U.S.A.* **1996**, *93*, 4425–4430.

(18) Henry, E. R.; Betatti, S.; Hofrichter, J.; Eaton, W. A. *Biophys. Chem.* **2002**, *98*, 149–164.

(19) Bruno, S.; Bonaccio, M.; Bettati, S.; Rivetti, C.; Viappiani, C.; Abbruzzetti, S.; Mozzarelli, A. *Protein Sci.* **2001**, *10*, 2401–2407.

(20) Nichols, W. L.; Zimm, B. H.; TenEyck, L. T. *J. Mol. Biol.* **1997**, *270*, 598–615.

(21) (a) Harada, I.; Takeuchi, H. In *Raman and Ultraviolet Resonance Raman Spectra of Proteins and Related Compounds, Advances in Spectroscopy*; Clark, R. J. H., Hester, R. E., Eds.; John Wiley & Sons: Chichester, 1986; pp 113−196. (b) Harada, I.; Miura, T.; Takeuchi, H. *Spectrochim. Acta* **1986**, *42A*, 307–312. (c) Miura, T.; Takeuchi, H.; Harada, I. *Biochemistry* **1988**, *27*, 88–94. (d) Miura, T.; Takeuchi, H.; Harada, I. *J. Raman Spectrosc.* **1989**, *20*, 667–671. (e) Matsuno, M.; Takeuchi, H. *Bull. Chem. Soc. Jpn.* **1998**, *71*, 851–857.

(22) (a) Rodgers, K. R.; Spiro, T. G. *Science* **1994**, *265*, 1697–1699. (b) Rodgers, K. R.; Su, C.; Subramaniam, S.; Spiro, T. G. *J. Am. Chem. Soc.* **1992**, *114*, 3697–3709.

(23) (a) Nagai, M.; Kaminaka, S.; Ohba, Y.; Nagai, Y.; Mizutani, Y.; Kitagawa, T. *J. Biol. Chem.* **1995**, *270*, 1636–1642. (b) Nagai, M.; Wajcman, H.; Lahary, A.; Nakatsukasa, T.; Nagatomo, S.; Kitagawa, T. *Biochemistry* **1999**, *38*, 1243–1251. (c) Nagai, M.; Imai, K.; Kaminaka, S.; Mizutani, Y.; Kitagawa, T. *J. Mol. Struct.* **1996**, *379*, 65–75.(d) Nagai, M.; Nagai, Y.; Aki, Y.; Imai, K.; Nagatomo, S.; Kitagawa, T. *XXIth Intl. Conf. Raman Spectrosc*, 2008; p 828. (e) Aki-Jin, Y.; Nagai, Y.; Imai, K.; Nagai, M. *ACS Symp. Ser.* **2007**, *963*, 297–311.

(24) Huang, S.; Peterson, E. S.; Ho, C.; Friedman, J. M. *Biochemistry* **1997**, *36*, 6197–6206.

(25) (a) Nagatomo, S.; Nagai, M.; Tsuneshige, A.; Yonetani, T.; Kitagawa, T. *Biochemistry* **1999**, *38*, 9659–9666. (b) Nagatomo, S.; Nagai, M.; Shibayama, N.; Kitagawa, T. *Biochemistry* **2002**, *41*, 10010–10020. (c) Nagatomo, S.; Jin, Y.; Nagai, M.; Hori, H.; Kitagawa, T. *Biophys. Chem.* **2002**, *98*, 217–232.

(26) (a) Kitagawa, T. *Prog. Biophys. Mol. Biol.* **1992**, *58*, 1–18. (b) Kitagawa, T.; Nagai, K.; Tsubaki, M. *FEBS Lett.* **1979**, *104*, 376–378.

(27) (a) Hu, X.; Spiro, T. G. *Biochemistry* **1997**, *36*, 15701–15712. (b) Hu, X.; Rodgers, K. R.; Mukerji, I.; Spiro, T. G. *Biochemistry* **1999**, *38*, 3462–3467. (c) Balakrishnan, G.; Case, M. A.; Pevsner, A.; Zhao, X.; Tengroth, C.; McLendon, G. L.; Spiro, T. G. *J. Mol. Biol.* **2004**, *340*, 843–856. (d) Balakrishnan, G.; Tsai, C. H.; Wu, Q.; Case, M. A.; Pevsner, A.; McLendon, G. L.; Ho, C.; Spiro, T. G. *J. Mol. Biol.* **2004**, *340*, 857–868. (e) Kneipp, J.; Balakrishnan, G.; Chen, R.; Shen, T. J.; Sahu, S. C.; Ho, N. T.; Giovannelli, J. L.; Simplaceanu, V.; Ho, C.; Spiro, T. G. *J. Mol. Biol.* **2006**, *356*, 335–353.

(28) (a) Peterson, E. S.; Friedman, J. M. *Biochemistry* **1998**, *37*, 4346–4357. (b) Huang, J.; Juszczak, L.; Peterson, E. S.; Shannon, C. F.; Yang, M.; Huang, S.; Vidugiris, G. V. A.; Friedman, J. M. *Biochemistry* **1999**, *38*, 4514–4525. (c) Kavanaugh, J. S.; Rogers, P. H.; Arnone, A.; Hui, H. L.; Wierzba, A.; DeYoung, A.; Kwiatkowski, L. D.; Noble, R. W.; Juszczak, L. J.; Peterson, E. S.; Friedman, J. M. *Biochemistry* **2005**, *44*, 3806–3820.

(29) (a) Aki, Y.; Nagai, M.; Nagai, Y.; Imai, K.; Aki, M.; Sato, A.; Kubo, M.; Nagatomo, S.; Kitagawa, T. *J. Biol. Inorg. Chem.* **2010**, *15*, 147–158. (b) Kaminaka, S.; Kitagawa, T. *Appl. Spectrosc.* **1992**, *46*, 1804–1808. (c) Haruta, N.; Aki, M.; Ozaki, S.; Watanabe, Y.; Kitagawa, T. *Biochemistry* **2001**, *40*, 6956–6963.

(30) (a) Balakrishnan, G.; Zhao, X.; Podstawska, E.; Proniewicz, L. M.; Kincaid, J. R.; Spiro, T. G. *Biochemistry* **2009**, *48*, 3120–3126. (b) Balakrishnan, G.; Ibrahim, M.; Mak, P. J.; Hata, J.; Kincaid, J. R.; Spiro, T. G. *J. Biol. Inorg. Chem.* **2009**, *14*, 741–750.

(31) (a) Dudik, J. M.; Johnson, C. R.; Asher, S. A. *J. Chem. Phys.* **1985**, *82*, 1732–1740. (b) Chi, Z.; Asher, S. A. *J. Phys. Chem. B* **1998**, *102*, 9595–9602.

(32) Gellin, B. R.; Karplus, M. *Proc. Natl. Acad. Sci. U.S.A.* **1977**, *74*, 801–805.

(33) (a) Chang, C.-k.; Simplaceanu, V.; Ho, C. *Biochemistry* **2002**, *41*, 5644–5655. (b) Mihailescu, M.-R.; Russu, I. M. *Proc. Natl. Acad. Sci. U.S.A.* **2001**, *98*, 3773–3777.

(34) (a) Perutz, M. F.; Kilmartin, J. V.; Nagai, K.; Szabo, A.; Simon, S. R. *Biochemistry* **1976**, *15*, 378–387. (b) Szabo, A.; Perutz, M. F. *Biochemistry* **1976**, *15*, 4427–4428.

(35) Rein, H.; Ristau, O.; Scheler, W. *FEBS Lett.* **1972**, *24*, 24–26.

(36) Salhany, J. M.; Ogawa, S.; Shulman, R. G. *Proc. Natl. Acad. Sci. U.S.A.* **1974**, *71*, 3359–3362.

(37) (a) Nagai, K.; Hori, H.; Yoshida, S.; Sakamoto, H.; Morimoto, H. *Biochim. Biophys. Acta* **1978**, *532*, 17–28. (b) Nagai, K.; Welborn, C.; Dolphin, D.; Kitagawa, T. *Biochemistry* **1980**, *19*, 4755–4761.

(38) Maxwell, J. C.; Caughey, W. S. *Biochemistry* **1976**, *15*, 388–396.

(39) Szabo, A.; Barron, L. D. *J. Am. Chem. Soc.* **1975**, *97*, 660–662.

(40) Scholler, D. M.; Wang, M.-Y. R.; Hoffman, B. M. *J. Biol. Chem.* **1979**, *254*, 4072–4078.

(41) Shibayama, N.; Morimoto, H.; Miyazaki, G. *J. Mol. Biol.* **1986**, *192*, 323–329.

(42) (a) Kikuchi, G.; Hayashi, N.; Yamamura, Y.; Enoki, Y.; Tyuma, I. *Biochim. Biophys. Acta* **1964**, *90*, 199–201. (b) Nishikura, K.; Sugita, Y.; Nagai, M.; Yoneyama, Y.; Jagenburg, R. *Nature* **1975**, *254*, 727–728. (c) Udem, L.; Ranney, H. M.; Bunn, H. F.; Pisciotta, A. *J. Mol. Biol.* **1970**, *48*, 489–498.

(43) (a) Nagai, K.; Kitagawa, T.; Morimoto, H. *J. Mol. Biol.* **1980**, *136*, 271–289. (b) Nagai, K.; Kitagawa, T. *Proc. Natl. Acad. Sci. U.S.A.* **1980**, *77*, 2033–2037.

(44) Fermi, G.; Perutz, M. F.; Shaanan, B.; Fourme, R. *J. Mol. Biol.* **1984**, *175*, 159–174.

(45) Park, S. Y.; Yokoyama, T.; Shibayama, N.; Shiro, Y.; Tame, J. R. *J. Mol. Biol.* **2006**, *360*, 690–701.

(46) Shaanan, B. *J. Mol. Biol.* **1983**, *171*, 31–59.

(47) Noble, R. W.; Hui, H. L.; Kwiatkowski, L. D.; Paily, P.; DeYoung, A.; Wierzba, A.; Colby, J. E. *Biochemistry* **2001**, *40*, 12357–12368.